BULGARIAN ACADEMY OF SCIENCES

CYBERNETICS AND INFORMATION TECHNOLOGIES • Volume **13**, No 2

Sofia • 2013

Print ISSN: 1311-9702; Online ISSN: 1314-4081
DOI: 10.2478/cait-2013-0017

A Software System for Classification of Archaeological Artefacts Represented by 2D Plans[1]

Valentin Hristov, Gennady Agre***

** Faculty of Mathematics and Informatics, Sofia University*
*** Institute of Information and Communication Technologies, 1113 Sofia*
Emails: valentine.hristov@gmail.com agre@iinf.bas.bg

Abstract: *The paper presents a method for representing whole and fragmented ceramic vessels depicted as two dimensional archaeological drawings. The process of construction of such a representation is described. It includes contour extraction from a vessel cross-section, splitting the contour into inner and outer profiles and converting them to tangent representation, is described. Some initial results of experiments, using the proposed representation for solving the task of identification of ancient Greek amphorae are discussed.*

Keywords: *2D image processing, curve representations, carve matching, ceramic profiles.*

1. Introduction

Ceramic artefacts are the most abundant of the archaeological findings. The study of these materials is very important in order to understand the culture, economic activity and the level of technological progress of the society that has produced these artefacts. An important part of archaeological analysis is the task for classifying ceramics based on the vessels' shape, their decoration, material, etc. The shape is one of the fundamental properties of a vessel used for its identification. However, the traditional shape descriptions rely on intuitive, often vague

[1] This paper is indexed with the support of Project No BG051PO001-3.3-05/0001 under the scheme "Science-Business" of the Operational Programme "Development of Human Resources".

characterizations, which are hard to quantify, or based on some easily measurable attributes (like vessel's height, diameter of its mouth, etc.), describing the vessel's shape only partially. In order to avoid the above mentioned subjectivity, more recent studies aiming at quantitative analyzing of ceramics try to achieve a formal (mathematical) description of the vessel shape by applying some image processing and pattern recognition methods to archaeological drawings of such vessels [13, 17, 8, 22]. In the general case an archaeological drawing is a manually made drawing, representing 2D sections, profiles or projections on selected planes of 3D objects (ceramic vessels of shards) (Fig. 1). The drawing content is not strictly standardized and relies on expert knowledge – for example, it can contain sketches of different details of a vessel (e.g., a handle or a bottom represented in different scales), ornaments, several cross-sections, etc.).

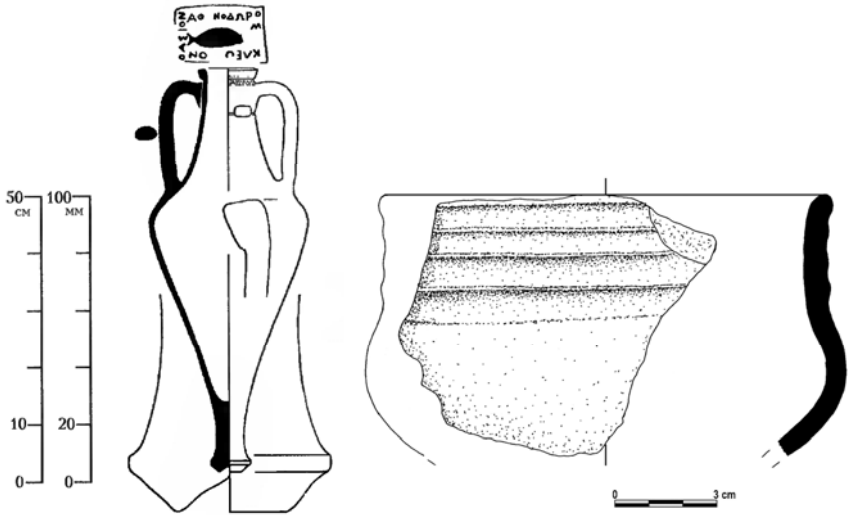

Fig. 1. Two examples of archaeological drawings

However, in most of the cases an archaeological drawing presents a vessel (or a shard) profile . The vessel consists of a curve which marks the vessel boundary or cross-section (that could be shown in the left or right part of the drawing), and a line which represents the central axis of rotation of the vessel. That is why the scanned drawings containing such elements are assumed to be an input to our system – the subject of this paper: the profile is used as a main source for constructing a formal representation of a vessel shape and the axis of rotation – for determining the relative dimensions of the vessel.

A vessel profile considered as a curve in the plain can be generally defined by coordinates $(x(s), y(s))$ of each of its points – the point moves along the curve as parameter s (arc-length) increases from 0 (initial point of the curve) up to L – the curve length. The small increments of the arc-length δs are related to the coordinate increments δx and δy by the formula $(\delta s)^2 = (\delta x)^2 + (\delta y)^2$, which is the base for computing the coordinates of the curve. The curve can be described by four different *representations* – Cartesian, polar, tangent and curvature [24] preserving

the complete information about the curve (excluding trivial shifts or rotation of the coordinated axes) (Fig. 2).

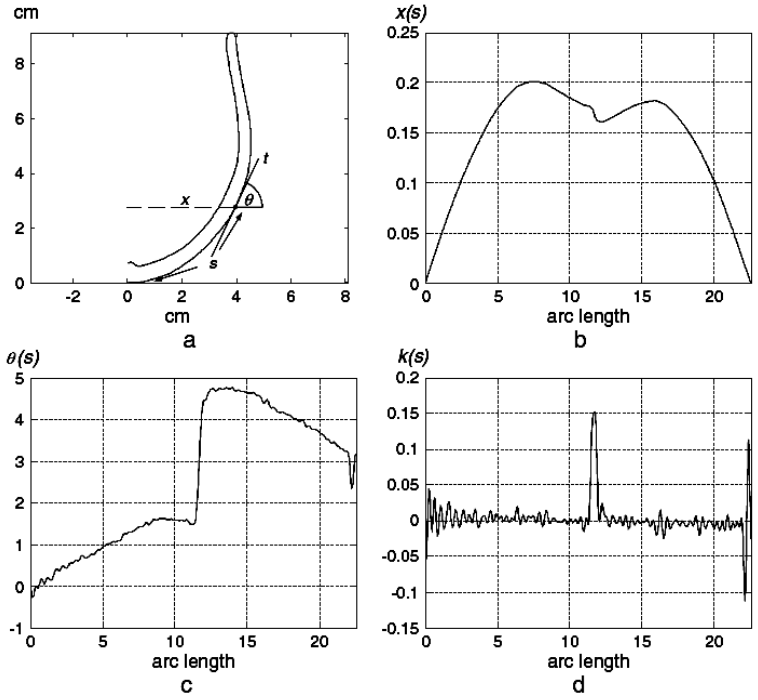

Fig. 2. A profile of a cup (a) and its representations: Cartesian (b), tangent (c) and curvature (d) [22]

The Cartesian and the polar representations provide the large-scale features of the curve – a small indentation that locally changes the curve will be represented as a small perturbation in these representations. The tangent representation, which is defined as a ratio of the derivatives of the Cartesian coordinates, is more dependent on the local changes along the curve. Since the curvature represents a derivative of the tangent angle, it is very sensitive to local variations and is not sensitive to the global properties of the curve [22]. The choice of a concrete representation depends on the particular task to be solved and assessment of what features of the curve are relevant for this task.

The representations of the vessel profile above mentioned have been used for solving different tasks constituting archaeological analysis. For example, the Cartesian and the tangent representations were used for solving a typological classification task [17, 13]; the curvature representation was widely used in different archaeological applications related to comparing artifacts based on their shapes [8, 10, 16, 19, 22]. The other techniques that could be used for description and comparison of ceramics include the Generalized Hough Transform [5, 14], Fourier transform [7], B-splines [12], etc.

The present paper describes some initial results related to the ongoing project aiming at developing a system facilitating archaeological analyses of artifacts based on their representation as 2D archaeological drawings. The emphasis is on the task of identification (classification) of ceramic vessels (or shards) which belong to a

discrete set of preliminary defined types (or classes). The input information for solving this task is a scanned drawing of pottery (from a book or an archaeological report) and an Internet-based database containing preliminary classified instances of vessels belonging to some vessel types.

The structure of the paper is as follows. The next section describes our method for representing a vessel profile. All preprocessing steps including detection of the axis of symmetry, separation of a cross-section, contour extraction, etc., are described in details. Section 3 explains how the constructed representation is used for comparing vessel shapes. Section 4 presents some experiments aiming at checking the applicability of the proposed approach for solving a classification task. As such pilot application the task for identification of ancient Greek amphorae found in the closed archaeological complexes on the territory of the Black sea coast was chosen. The last section is devoted to the discussion of the experiment results and presents our intentions for further development of the system.

2. Representing profiles

As it has already been mentioned, the comparison of two ceramic objects in our system is based on calculating the similarity between objects' profiles. The representation of profiles should allow the solution of the following tasks:

- Comparing profiles of whole vessels;
- Comparing the profile of a shard against the profile of a whole vessel;
- Comparing profiles of shards.

In general, the first two tasks can be considered as an instance of a more general task "whole-to-part matching" [3], in which one curve is assumed to be potentially embedded into another. To solve this task it is necessary to find a position, where the first (shorter) curve aligns to the second curve. The third task is an instance of the so called "part-to-part matching" problem, in which the best matching parts of two curves should be found. Naive solutions of both general tasks have time complexity of $O(N^3)$ [3], where N is the number of points representing the longer curve. That is why, at the moment we have simplified the tasks by assuming that the starting (initial) points of the profiles to be compared should be the same. This assumption restricts the types of ceramic fragments which can be processed by the system to top (containing the rim) or bottom fragments of a vessel. Deleting fragments of a vessel body is not a too high price since in most cases the archaeologists consider them as minimally informative [8].

In order to allow comparing profiles of shards against profiles of whole vessels, the representation of a whole vessel profile should contain two initial points – one for comparing fragments containing the rim, and another – for comparing fragments containing the bottom. The next sections describe the process of constructing the profile representation in more details.

2.1. Extracting the vessel profile

A profile is a contour of a vessel cross-section and should be first extracted from the scanned drawing of the vessel. As input data our system accepts grey-scale images

in any of the popular formats – JPEG, PNG, GIF and TIFF. The image should contain an archaeological drawing of a vessel (or a fragment) with clearly shown cross-section and a central axis of symmetry. The minimal required resolution of the image is 300 DPI. The extraction of a vessels' profile consists of a sequence of pre-processing steps. Their goal is to make the input image to meet some formal requirements (e.g., the central axis should be at 90 degrees, etc.) that have been already described earlier, and to extract certain properties of the profile that will be used later in the profile comparison process. The pre-processing includes binarization, some morphological operations, segmentation and scaling of the image.

- *Binarization:* usually the profiles are drawn with a pencil on white paper and then transferred into a digital format through scanning. Some of the image processing algorithms that we use work with binary images and do not use the information of the profile colour. That is why the input image is converted into a binary format using Otsu's method [21].
- *Reflection:* the system requires that the cross-section of the profile is on the left hand side of the image. If the cross-section is not found at the correct side of the image, the reflection operation [24] is automatically applied to flip the image. To detect whether the profile is oriented correctly, the input image is split vertically in two parts as the axis of symmetry of the object is selected as a split line. The side with more black pixels is assumed to be the side of the cross-section.
- *Detecting the axis of symmetry:* the axis of symmetry of a profile is usually the longest straight line in the image. Its position is found by applying Hough transform [4, 11]. The axis of symmetry is used to calculate automatically the scale factor of the image. This is done by measuring the distance from the left-most point of the rim of the vessel to the x coordinate of the axis.
- *Separating the cross-section:* the next step consists in finding the edges of the cross-section. In order to achieve this we have to overcome the problem that the cross-section is often drawn connected with the other parts of the vessel (see Fig. 3). To remove these connections we apply such morphological operations as erosion (two or three times depending on the thickness of the connection lines), and then the same number of dilatations (this operation is called "opening" when the erosion and the dilatation are applied only once [25]). The effect of these operations is that the (enough) thin lines are practically erased from the image. This approach gives good results when the connection lines are not very thick (three to six pixels); otherwise the erosion alters the cross-section of the profile too much before the connection lines disappear and even the application of dilatation could not recover the initial shape of the cross-section. In such cases the system provides the user with the option to erase the connecting lines manually.
- *Edge detection*: after separating the cross-section, the edges should be detected. We do not use the classical edge detection algorithms (such as Sobel, Canny, "thresholding and linking", etc.) for two reasons:

1. We would like to find not only the image contour but to detect the different regions of the drawings as well. One such region is the vessel cross-section, but

the drawings can have others objects (like a stamp of the amphora maker, a cross-section of the vessel handle, etc) that could also be used for analyzing the vessel.

2. These algorithms are unnecessarily complex for processing a simple binary image. That is why an algorithm similar to the one described in [2], which combines the concept of sequential region labelling and traditional contour tracing into a single step, has been chosen. After storing the contour as a sequence of pixels, the representation of the contour is created.

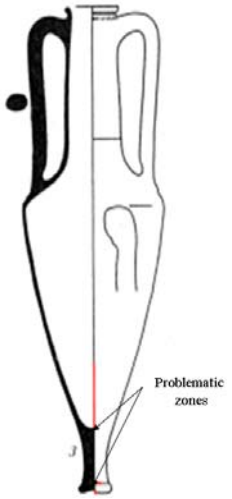

Fig. 3. Problematic connections

2. 2. Creating a profile representation

A profile is represented by means of the modified Freeman chain code, which is a discrete representation of the mutual position of every two neighboring pixels belonging to the vessel profile edges. The standard chain code quantizes the position of the adjacent pixels into one of eight directions. Since this approximation to the real tangent angle is too rough, the modification of the chain code [16] is used in order to minimize the quantization error. At the first step the contour of the cross-section is transformed into a Freeman chain code representation [6, 1] – a vector of integers, where each entry corresponds to the discrete angle formed by the adjacent pixels. The contour pixels are traversed in a fixed counter-clockwise direction. Due to the nature of the square sampling lattice, the chain code angles are constrained to a discrete range of eight values (0, …, 7) representing multiples of 45°.

The second step aims at correcting some quantization errors inherent from the chain code definition:

1. The angle quantization within the range from 0 up to 7 may introduce discontinuities of more than 180° (e.g., when 7 follows after 0). To avoid this, modulo 8 operation putting a bound on the angle discontinuities is applied.

2. The presence of a discretization error caused by the fact that in real world the diagonal of a unit square is $\sqrt{2}$, whereas in our discrete sampling lattice this distance between the adjacent pixels is equal in all directions. This problem is

solved by counting three length units for pixels in diagonal direction and two length units for pixels in horizontal and vertical direction.

At the third step the modified chain code $\theta(s)$ is corrected again in order to solve amplification problems occurring when differentiating a discrete signal, such as $\theta(s)$ [16]. The signal is filtered by a standard Gaussian template with kernel 7.

2.3. Improved representation of a profile

The improved representation of a profile is to facilitate the finding of solutions for the three tasks defined at the beginning of this section – comparing profiles of whole vessels; comparing profiles of shards with profiles of whole vessels, and comparing profiles of shards. The improvement does not depend on the concrete representation chosen for defining profiles – the Cartesian, the tangent or the curvature. It concerns the selection of initial and ending points of a profile according to the type of the object described by this profile – the whole vessel, the top fragment (containing a part of the vessel rim) or the bottom fragment.

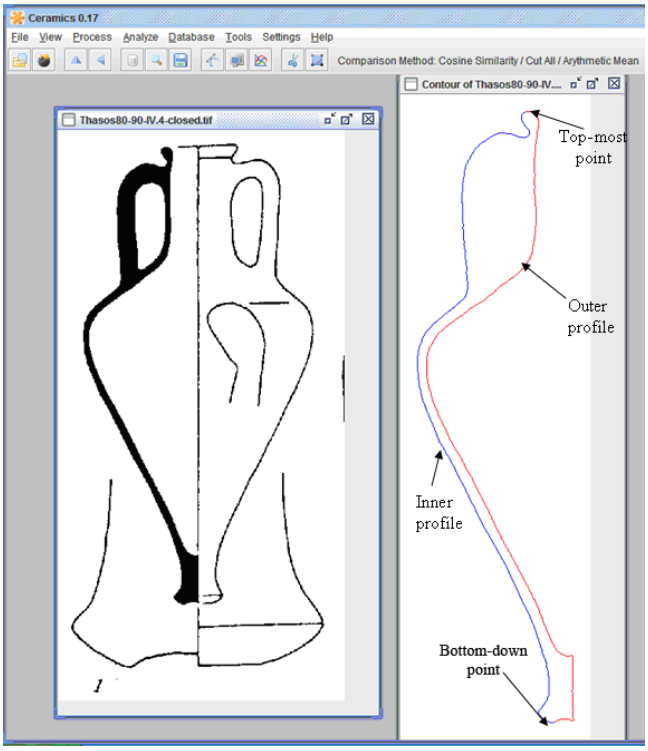

Fig. 4. Left-oriented cross section and its contour

As it has already been mentioned we assume that the vessel cross-section is located always on the left side of the drawing, as shown in Fig. 4. This condition is formal and represents the way the profiles are stored in our system database. It does not enforce any restrictions on the input data since the profile could be easily oriented in the correct direction using the mathematical operation “reflection”. In

the case of a whole vessel, the profile is represented by two points – the first one is the top-most point of the profile, and the second – the bottom-down point. The top-most point is the first point from the profile found when traversing the image line by line from left to right and from top to bottom. This point is used as the starting (initial) point when comparing whole vessels, top fragments with whole vessels and one top fragment against another top fragment.

The bottom-down point of a profile is the first point found when traversing the image line by line from right to left and from bottom to top. This point is used as the starting (initial) point when comparing bottom fragments or bottom fragments with whole vessels.

The top-most and the bottom-down points split a whole vessel profile in two parts – the inner profile and the outer profile (see Fig. 4). All points of the profiles, when it is traversed in clockwise direction from the top-most point to the bottom-down point, are marked as inner points. Correspondently, all points of the profile lying between the bottom-down point and the top-most point, when the profile is traverse in clockwise direction, are marked as outer. So the bottom-down point is considered as the ending point of the inner profile and the top-most point – as the ending point of the outer profile of the whole vessel. In this way the similarity between two whole vessels is calculated as average similarity between their inner and outer profiles.

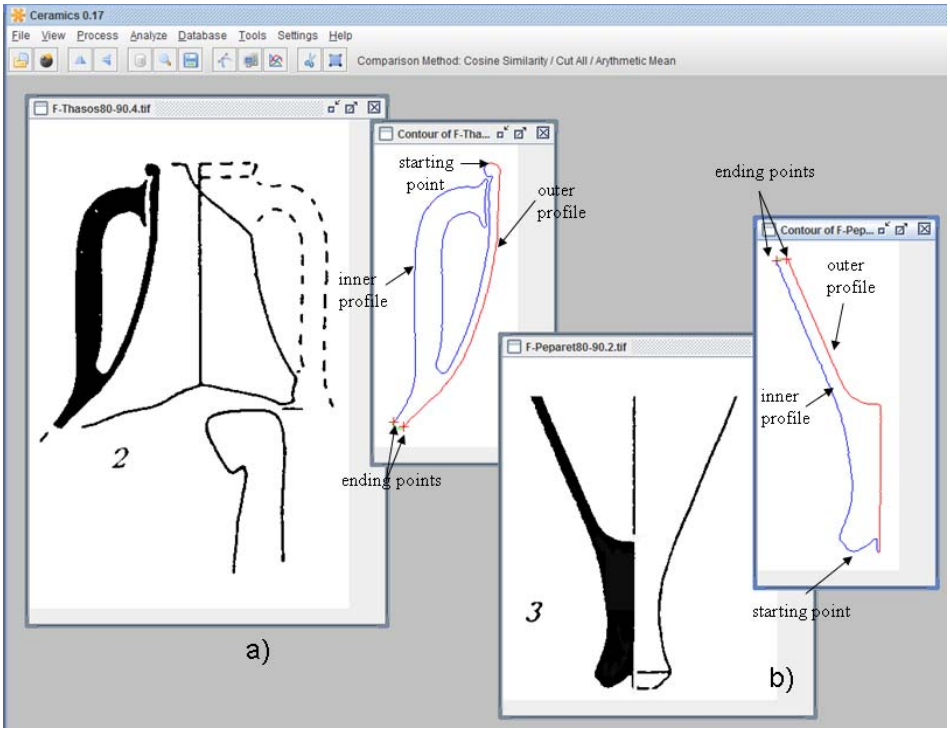

Fig. 5. Inner and outer profiles of shards: top fragment (a); bottom fragment (b)

In the current implementation we have restricted the shards that can be processed by the system to two types – bottom and top fragments. The starting point

of a top fragment is defined by its top-most point and the starting point of a bottom fragment – by its bottom-down point. The main problem with processing shard profiles is that it is necessary to exclude the curve connecting their break points from the description of the profiles. We have solved this problem by allowing the user to mark such points in the picture of the extracted profile of a shard (see Fig. 5). The specified points, which are marked by red crosses in Fig. 5, are considered as ending points of the shard profile. In order to determine the inner and the outer profiles of a shard, its contour is traversed twice always starting from the initial point – once in the clockwise direction and once – in the counter-clockwise direction. In the case of a top fragment all points lying between the starting point and the first encountered break point, when traversing in the clockwise direction, are marked as inner ones, and those found when traversing in the counter-clockwise direction – as outer ones. In the case of a bottom fragment the inner profile is formed by the points traversing in the counter-clockwise direction and the outer – those from the clockwise direction. The points of the contour that are marked neither as inner nor as outer are excluded from the profile description.

3. Comparing profiles

In our system a profile is represented by a triple:

(1) $$\boldsymbol{\theta}(s) = \langle T, \boldsymbol{\theta}_{\text{inn}}(s), \boldsymbol{\theta}_{\text{out}}(s) \rangle,$$

where:

T denotes the profile type: whole, top fragment or bottom fragment;

$\boldsymbol{\theta}_{\text{inn}}(s) = \{\theta_{\text{inn}}(1), \ldots, \theta_{\text{inn}}(n)\}$ – a discrete tangent representation of the inner profile; n – number of points in the profile;

$\boldsymbol{\theta}_{\text{out}}(s) = \{\theta_{\text{out}}(1), \ldots, \theta_{\text{out}}(m)\}$ – a discrete tangent representation of the outer profile; m – number of points in the profile.

In the case of a whole vessel the initial point of the inner profile coincides with the ending point of the outer profile and vise versa:

if T = whole: $\theta_{\text{inn}}(1) = \theta_{\text{out}}(m)$; $\theta_{\text{out}}(1) = \theta_{\text{inn}}(n)$.

In the case of shards, the initial points of the inner and outer profiles are the same ($\theta_{\text{inn}}(1) = \theta_{\text{out}}(1)$) and coincide with either the top-most point (if the shard is a top fragment) or with the bottom-down point (if the shard is a bottom fragment).

Similarity between two profiles $\boldsymbol{\theta}^A(s)$ and $\boldsymbol{\theta}^B(s)$ is defined as a weighted average similarity between the inner and the outer profiles of compared objects:

(2) $$\text{sim}(\theta^A(s), \theta^B(s)) = \frac{w_{\text{inn}}\text{sim}(\theta^A_{\text{inn}}(s), \theta^B_{\text{inn}}(s)) + w_{\text{out}}\text{sim}(\theta^A_{\text{out}}(s), \theta^B_{\text{out}}(s))}{w_{\text{inn}} + w_{\text{out}}},$$

where the non-negative coefficients w_{inn} and w_{out} reflect the importance of the similarity between the corresponding parts of the object profiles.

Since the tangent representation of a curve is invariant with respect to the similarity transform, as a measure of similarity between vectorized representations of two profiles we have selected a simple correlation coefficient [23]. However, before calculating the correlation, the following three problems should be solved:

1. *The compared vectors should start from the same point* – when profiles of whole vessels are compared, the starting points of the inner and outer profiles of both vessels are identical. The same is true when two shards belonging to the same type (bottom or top fragments) are compared. The correspondence should be made only when comparing the profiles of a shard with the profiles of a whole vessel – in the case of a top fragment the vector representing the outer profile of the whole vessel should be "reversed" before comparing, i.e., its ending point should become the starting point and its starting point – the ending point. When a bottom fragment is compared, the same "reverse" transformation should be applied to the inner profile of the whole vessel used in the comparison.

2. *The compared vectors should be of the same dimension* – this problem is easily solved by using the shorter curve as a template and trimming all attributes of the longer vector that correspond to the points lying after the last point of the shorter vector.

3. I*t should be guaranteed that the comparison of two curves is carried out in points that always lie at the same distances from the starting points of both curves*. This problem is caused by the discrete representation of a curve since the arc-length between two successive points of a curve depends on the scale used to drawing it. We have solved this problem by transforming all archaeological drawings of vessels to a "standardized form" using information about the "vessel radius" – the distance from the starting point of the vessel profile up to its axes of symmetry. Before starting the procedure for extracting the object contour, the drawing is automatically scaled to the standard form which has a constant "vessel radius" (in our experiments the radius was equal to 100 pixels). In this way we have ensured that the profiles of all objects stored in the system database are represented in the same scale.

Assuming that the above mentioned problems have been solved, the similarity between two curves A and B described by their tangent representations $\theta A(s) = \{\theta A(1), \ldots, \theta A(n)\}$ and $\theta B(s) = \{\theta B(1), \ldots, \theta B(m)\}$ is calculated as:

$$\text{sim}(\theta_A, \theta_B) = \frac{\sum_{i=1}^{k} \theta_A(i)\theta_B(i)}{\sqrt{\sum_{i=1}^{k} \theta_A^2(i)}\sqrt{\sum_{i=1}^{k} \theta_B^2(i)}}, \quad k = \min\{n, m\}. \tag{3}$$

The classification of an unknown object is done by comparing it to preliminary classified vessels (or shards) stored in the system database, The comparison is done by means of a standard *k*-nearest neighbour algorithm which uses the similarity measure defined by formulae (2) and (3).

4. Experiments

In order to check the applicability of the above described approach we have selected the task for identification of ancient Greek amphorae found in the closed archaeological complexes on the territory of the Black sea coast. These complexes contain amphorae produced in different ancient Greek centers, such as Thasos, Menda, Heraclea, Knid, Hios, etc. We have restricted the task to amphorae which

date back to IV century BC (Fig. 6). As an input to the system we have used scanned drawings of amphorae given in the book of M o n a h o v [20]. Although the original drawings were made in scale 1:10 cm, the size of the scanned drawings depends on the size of the book page on which they are shown; thus, in practice, in the experiments we have used drawings of amphorae represented in different scales. The drawings were scanned with 300 DPI resolution and the average size of a scanned drawing varied between 90 KB and 750 KB.

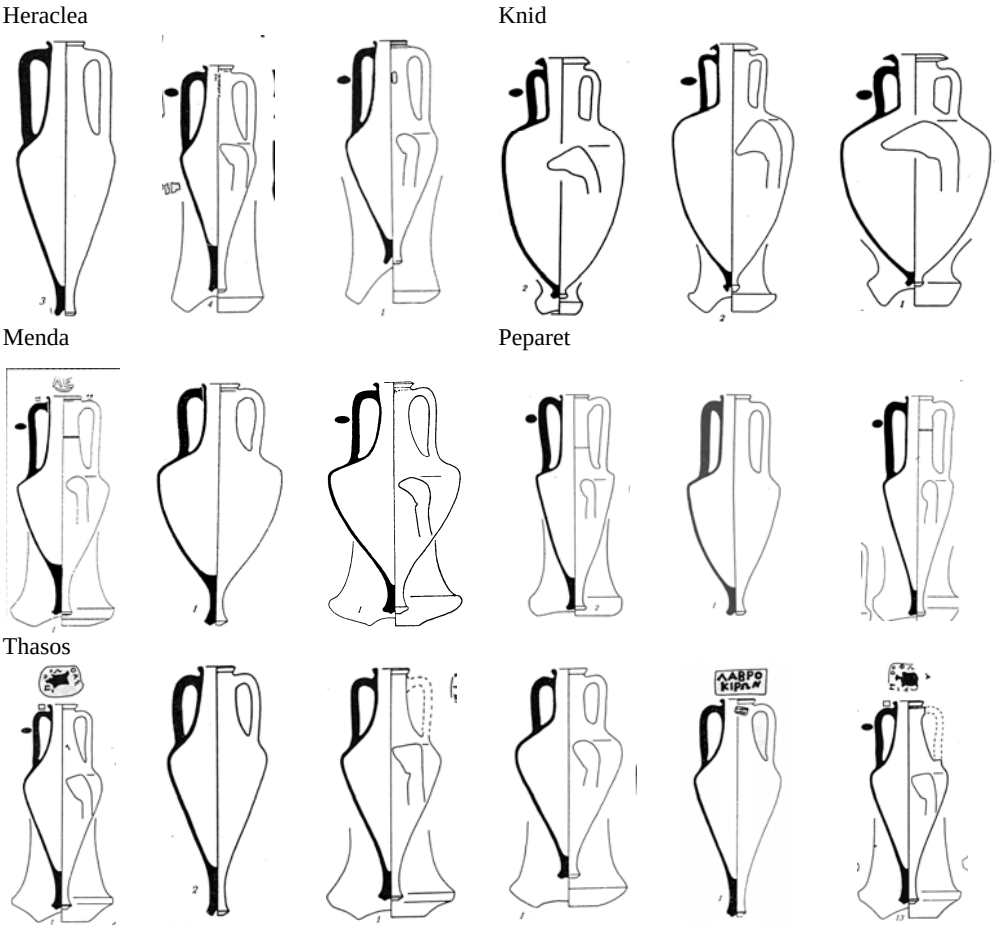

Fig. 6. Examples of whole amphora drawings used in the experiments

In the first experiment we have used 71 drawings of whole amphorae distributed into five classes according to their centers of production (Table 1).

Table 1. Distribution of examples of whole amphora drawings among the classes

Class	Heraclea	Menda	Peparet	Thasos	Knid
Number	20	13	13	22	3

All drawings have been processed by the system and the tangent representations of the drawings have been saved in the system database. The classification accuracy was evaluated by means of the nearest neighbor algorithm

applied in the Leave-one-out cross-validation schema [18]. The accuracy obtained in this experiment was 73.0 %.

The second and the third experiments aimed at evaluating the potential of the tangent representation of amphorae profiles for solving the task of comparing drawings of amphora fragments with drawings of whole amphorae (Fig. 7). In these experiments we have used 34 top fragments and 15 bottom fragments of amphorae belonging to the five classes above mentioned (Table 2).

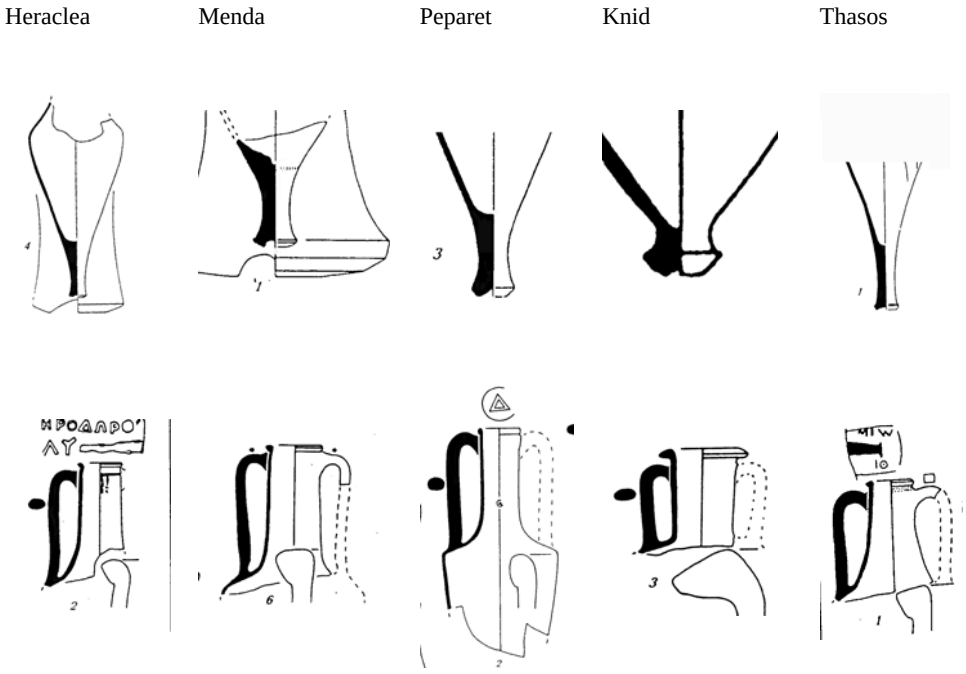

Fig. 7. Examples of drawings of amphora fragments used in the experiments

After processing all drawings, the tangent representation of each fragment was compared with the tangent representations of 71 drawings of whole amphorae by the nearest neighbor algorithm. The obtained classification accuracy in classifying the bottom fragments was 73.3 % and 70.6 % – for the top fragments.

Table 2. Distribution of examples of fragmented amphora drawings among the classes

Class	Heraclea	Menda	Peparet	Thasos	Knid
Top Fragments	2	3	7	2	1
Bottom Fragments	8	6	5	12	3

5. Discussion and future work

The results of the experiments show that the developed representation of pottery profiles allows the implementation of a unified approach to solving the classification tasks related to the identification of whole vessels and to the

identification of their characteristic fragments. This approach can be considered as further development of the ideas proposed in [8]. The obtained classification accuracies in all three experiments are significantly higher than the accuracy of a default classifier (i.e., the classifier that always classifies an unknown object to the prevailing class). The relatively similar results achieved in all experiments confirm the statement made by the archaeologists that the shape of the vessel rim and the shape of the bottom have major contribution for identifying the pottery. However, the obtained accuracies could not be considered as satisfactory enough. The possible reasons for this are as follows:

- Low quality of the drawings used for creating the database containing examples of standard vessels – as it has been already mentioned those drawings had small dimensions and were scanned with a relatively low resolution. As a result some important details related to the shape of the vessel rims and bottoms were not presented clearly enough.
- Potential deformations of vessel profiles caused by the application of such morphological operations, such as erosion and dilatation that had to be carried out by the user in order to separate a vessel cross-section. Having in mind that these operations were applied mainly to the parts of drawings depicting the vessel bottoms, which had been proved to play a very important role in the vessel identification process, the potential changes in their shapes could significantly affect the evaluation of vessels similarity. Another argument in the same direction is that there is not any common archaeological standard in depicting amphorae – in some drawings the cross-section of an amphora handle was depicted as a fully connected part of the whole vessel cross-section, while in others this connection was broken in the upper part of the handle. Such a small detail causes absolutely different in shape profile representations. In order to avoid this deficiency we had to fill (or disjoint) the corresponding part of each drawing in order to obtain a unified representation for all amphora drawings. Of course, such interventions could be a source of potential distortions of the original shape of an amphora. A potential solution of the problems above mentioned is the development of a new standard for drawing amphorae that is suitable for automatic extraction of amphora profiles from drawings.
- Transformation of the drawings into a standard form is a practical solution of the problem concerning the use of different scales in the drawings. However, such a transformation adds additional “noise” to a pixelated version of the contour, especially in cases when the initial drawing has a small size and is of low quality. The applied smoothing procedure could not completely compensate such noise since its parameters are fixed and cannot be dynamically adjusted.
- Of course, we could not reject also the hypothesis that the tangent representation chosen for describing the profiles, is not sufficiently sensitive for solving the amphorae identification task, that was selected as a pilot application of the system.

Based on the detailed analysis of the above described initial experiments with the system, we are going to continue our work in the following main directions:

- *Improving the internal representation of pottery profiles*: as a promising candidate for such representation we consider the scale invariant signature that is based on integral of the curvature [3] – a comparatively new approach for solving the general problem of matching open curves. This representation does not need the application of any preliminary standardization (rotation and scaling) procedures. Moreover, it would allow us to apply an arc-length step of adjustable size used for comparing profiles by automatically selecting smaller steps in such places of the profile where its shape is changed more sharply (i.e., the rim and the bottom) and bigger steps for parts where this occurs slightly.
- *Improving the template matching algorithm*: instead of the simple correlation coefficient that is currently used for comparing vessel profiles, we are going to apply the normalized cross correlation measure [15]. This measure along with a slight modification of the currently used representation of a profile as a triple, including the inner and the outer profiles of the cross-section, will allow us to extend the type of ceramic fragments that can be processed by the system to body-shards as well.
- *Improving the classification algorithm:* the *k*-nearest neighbour method that is currently used for classifying ceramic objects is a very simple and efficient algorithm. However, it has an essential (for the task of ceramic vessel identification) defect – it does not allow easy identification of a test object as not belonging to any of the known classes. In order to avoid this problem, we are going to apply a variant of the Reduced Coloumb Energy Network [4], which classifies an object as unknown if it falls out of all hyperspheres centred in the training examples that are implemented by means of hidden nodes of the network.

Acknowledgement: The work on this paper was partially supported by EC FP7-REGPOT-2012-2013-1 Project "AComIn: Advanced Computing for Innovation".

References

1. Burger, W., M. J. Burge. Digital Image Processing, An Algorithmic Introduction Using Java. Springer, 2008.
2. Chang, F., C. J. Chen, C. J. Lu. A Linear-Time Labelling Algorithm Using Contour Tracing Technique. – Computer Vision and Image Understanding, Vol. **93**, February 2004, Issue 2, 206-220.
3. Cui, M., J. Femiani, J. Hu, P. Wonka, A. Razdan. Curve Matching for Open 2D Curves. – Pattern Recognition Letters, Vol. **30**, 2009, 1-10.
4. Duda, R., P. Hart, D. Stock. Pattern Classification. Second Edition. John Willy and Sons, Inc, 2001.
5. Durham, P., P. Lewis, S. Shennan. Artefact Matching and Retrieval Using Generalised Hough Trasform. – In: I. Wilcock, K. Lockyear, Eds. Computer Applications and Quantitative Methods in Archaeology, 1993, BAR Int. Ser. 598, 1995, 25-30.
6. Freeman, H. On the Classifcation of Line Drawing Data. – In: W. Wathen-Dunn, Ed. Models for the Perception of Speech and Visual Form. Cambridge, MA, MIT Press, 1967, 408-412.
7. Gero, J., J. Mazullo. Analisys of Artifact Shape Using Fourie Series in Closed Form. – Journal of Field Archaeology, Vol. **11**, 1984, No 3, 315-322.
8. Gilboa, A., A. Karasik, I. Sharon, U. Smilansky. Towards Computerized Typology and Classification of Ceramics. – Journal of Archaeological Sciences, Vol. **31**, 2004, 681-694.

9. Gonzales, R. C., R. E. Woods. Digital Image Processing. Second Edition, Prentice Hall, 2002.
10. Hagstrum, M. B., J. A. Hildebrand. The "Two-Curvature" Method for Reconstructing Ceramic Morphology. – American Antiquity, Vol. **55**, 1990, No 2, 388-403.
11. Illingworth J., J. Kittler. A Survey of the Hough Transform. – Computer Vision, Graphics and Image Processing, Vol. **44**, 1988, 87-116.
12. Kampel, M., R. Sablating. Fitting of a Close Planar Curve Representing a Profile of an Archaeological Fragment. – In: Proc. of the 2001 Conference on Virtual Reality, Archaeology, and Cultural Heritage, 2001, 263-269.
13. Leese, M. N., P. L. Main. An Approach to the Assessment of Artifact Dimension as Descriptors of Shape. – In: J. G. B. Haigh, Ed. Computer Applications in Archaeology. University of Bradford, School of Archaeological Sciences, Bradford, 1983, 171-180.
14. Lewis, P. H., K. J. Goodson. Images, Databases and Edge Detection for Archaeological Object Drawings. – In: K. Lockyear, S. Rahtz, Eds. Computer Applications and Quantitative Methods in Archaeology 1990, 1991, 149-152.
15. Lewis, J. P. Fast Normalized Cross-Correlation. – In: Vision Interface, Canadian Image Processing and Pattern Recognition Society, 1995, 120-130.
16. Leymarie, F., M. D. Levine. Curvature Morphology. Computer Vision and Robotics Laboratory. Montreal, Quebec, McGill University, 1988.
17. Limming, G., L. Hongjie, J. Wilcock. The Analysis of Ancient Chinese Pottery and Porcelain Shapes: A Study of Classical Profiles from Yangshao Culture to the Qing Dynasty Using Computerized Profile Data Reduction, Cluster Analysis and Fuzzy Boundary Discrimination. – In: Computer Applications and Quantitative Methods in Archaeology, 1989, 363-374.
18. Mitchell, T. Machine Learning. McGraw Hill, 1997.
19. Mokhtarian, F., M. Bober. Curvature Scale Space Representation and MPEG-7 Standartization 25. The Netherlands, Kluwer Academic Publishers, 2003.
20. Monahov, S. Greek Amphorae from Black See Coast. Saratov University Publ., 1999 (in Russian).
21. Otsu, N. A Threshold Selection Method from Gray-Level Histograms. – IEEE Transaction on Systems, Man, and Cybernetics, Vol. **SMC-9**, January 1979, No 1, 62-69.
22. Saragusti, I., A. Karasik, I. Sharon, U. Smilansky. Quantitative Analysis of Shape Attributes Based on Contour and Section Profiles in Artifact Analysis. – Journal of Archaeological Science, Vol. **32**, 2005, 841-853.
23. Sincich, T. Statistics by Example. Forth Edition. San Fransisco, Dellen Publ. Company, 1990.
24. Smith, P. F., A. S. Gale. Introduction to Analytical Geometry. Ginn & Company, 2009.
25. Scot, U., R. C. Gonzales. Computer Vision and Image Processing, NJ, Prentice Hall, 1998.